



Cite this: DOI: 10.1039/c5fo01475a

Morinda citrifolia edible leaf extract enhanced immune response against lung cancer

Swee-Ling Lim,^a Yong-Meng Goh,^b M. Mustapha Noordin,^b Heshu S. Rahman,^a Hemn H. Othman,^b Nurul Ain Abu Bakar^a and Suhaila Mohamed^{*a}

Lung cancer causes 1.4 million deaths annually. In the search for functional foods as complementary therapies against lung cancer, the immuno-stimulatory properties of the vegetable *Morinda citrifolia* leaves were investigated and compared with the anti-cancer drug erlotinib. Lung tumour-induced BALB/c mice were fed with 150 mg kg⁻¹ or 300 mg kg⁻¹ body weight of the leaf extract, or erlotinib (50 mg kg⁻¹ body-weight) for 21 days. The 300 mg kg⁻¹ body weight extract significantly (and dose-dependently) suppressed lung tumour growth; the extract worked more effectively than the 50 mg kg⁻¹ body weight erlotinib treatment. The extract significantly increased blood lymphocyte counts, and spleen tissue B cells, T cells and natural killer cells, and reduced the epidermal growth factor receptor (EGFR) which is a lung adenocarcinoma biomarker. The extract also suppressed the cyclooxygenase 2 (COX2) inflammatory markers, and enhanced the tumour suppressor gene (phosphatase and tensin homolog, PTEN). It inhibited tumour growth cellular gene (transformed mouse 3T3 cell double minute 2 (MDM2), V-raf-leukemia viral oncogene 1 (RAF1), and mechanistic target of rapamycin (MTOR)) mRNA expression in the tumours. The extract is rich in scopoletin and epicatechin, which are the main phenolic compounds. The 300 mg kg⁻¹ *Morinda citrifolia* leaf 50% ethanolic extract showed promising potential as a complementary therapeutic dietary supplement which was more effective than the 50 mg kg⁻¹ erlotinib in suppressing lung adenocarcinoma. Part of the mechanisms involved enhancing immune responses, suppressing proliferation and interfering with various tumour growth signalling pathways.

Received 1st December 2015,
Accepted 8th December 2015

DOI: 10.1039/c5fo01475a

www.rsc.org/foodfunction

Introduction

Lung cancer is the leading cause of cancer-related deaths worldwide, with 1.6 million new cases and 1.4 million deaths per year. Non-small-cell lung cancer (NSCLC) accounts for approximately 85% of all lung cancer cases, with a 5-year survival rate of only 16%.¹ Chemotherapy is relatively ineffective for patients with advanced NSCLC and the response rate is only 20% to 35% with a median survival of 10 to 12 months.² In a phase III study, the use of epidermal growth factor receptor (EGFR) tyrosine kinase inhibitor (TKI) drugs, such as erlotinib, significantly improved the overall survival rate relative to supportive care for refractory stage IIIB/IV NSCLC. However, erlotinib use is limited because of several serious side effects³ and the emergence of cancer mutations which confer drug resistance. The common erlotinib side effects are weakness, diarrhoea, rashes, shortness of breath, coughing, loss of appetite,

fatigue (feeling tired), and nausea. Erlotinib may cause more serious side effects such as lung problems (shortness of breath, coughing, and fever); interstitial lung disease and liver and kidney problems; blistering and skin peeling; gastrointestinal perforation; bleeding and clotting problems which may lead to heart attacks, strokes, dry eyes, unusual eyelash growth, or swelling of the corneas; harm to unborn babies and even death.

The inflammatory process and cyclooxygenase 2 (COX2) are important contributors to lung cancer development and pathogenesis. NSCLC is often accompanied by increased COX2 expression,⁴ which catalyzes the conversion of arachidonic acid into the unstable intermediate prostaglandin H₂, to form other prostanoids: prostaglandin (PG)-E₂, prostacyclin and thromboxane (Tx)-A₂. The COX2 expression correlates positively with a poor prognosis stage I disease and increased COX2 mRNA levels foretell a low survival rate from NSCLC.⁵

Morinda citrifolia (Rubiaceae) leaves are commonly consumed as vegetables after blanching by the Polynesians of South East Asia. The *M. citrifolia* leaves also have some healing properties and are traditionally used to treat wound infections, pain, arthritis, swellings, and similar conditions. *M. citrifolia* leaves have antioxidant, liver-protective and wound restorative effects⁶ without any acute, sub-acute and sub-chronic oral

^aUPM-MAKNA Cancer Research Laboratory, Institute of Bioscience, University Putra Malaysia, 43400 Serdang, Selangor, Malaysia.

E-mail: mohamed.suhaila@gmail.com; Fax: +603-8947-2101; Tel: +603-8947-2168

^bFaculty of Veterinary Medicine, Universiti Putra Malaysia, 43400 Serdang, Selangor, Malaysia

toxicity.⁷ An oral intake of 1000 mg kg⁻¹ of *M. citrifolia* leaf ethanolic extract has been reported as the no observed-adverse-effect level (NOAEL).⁸ This study attempts to investigate the possible immune-stimulatory and tumour suppressive effects of *M. citrifolia* edible leaves as a complementary therapy against lung cancer and compare it to erlotinib.

Experimental

Plant materials

The *M. citrifolia* leaves (voucher no. SK2322/14, identified by Biodiversity Unit, Institute of Bioscience, University Putra Malaysia, Serdang) were collected from Institute of Bioscience, University Putra Malaysia, State of Selangor, Malaysia. The leaves were dried and mixed in a ratio (w/v) of 1 : 5 with 50% ethanol in water. The yield was 13.61%. The extracts were analyzed using high-performance liquid chromatography, HPLC (Waters 2996, Milford, MA).⁹ HPLC grade methanol (MeOH), acetonitrile (MeCN) and analytical grade trifluoroacetic acid (TFA) were obtained from Merck (Darmstadt, Germany).

Chemical characterisation and standardisation of the 50% ethanolic leaf extract

The leaf extract was analysed using high pressure liquid chromatography with an Atlantis C18 column (4.6 mm × 250 mm; 5 µm, Waters Corporation, Milford, MA, USA), maintained at 25 °C. The mobile phase consisted of three solvents: A; MeCN, B; MeOH, and C; 0.1 TFA% in H₂O (v/v), programmed consecutively in linear gradients as follows: 0 min, 10% A, 10% B, and 80% C; 15 min, 20% A, 20% B, and 60% C; 26 min, 40% A, 40% B, and 20% C; 28–39 min, 50% A, 50% B, and 0% C; and 40–45 min, 10% A, 10% B, and 80% C. The elution was run at a flow rate of 1.0 mL min⁻¹ with a 50 µL sample injection volume, and a UV spectra detector set at 210 and 450 nm. The extract contained 2.19% scopoletin (retention time, *R*_t = 12.02 min) and 3.41% epicatechin (*R*_t = 9.17 min) as the main compounds, which were qualitatively and quantitatively identified *via* the retention times and calibrated standard plots. Spiking with scopoletin and epicatechin produced sharp extended peaks at the specific retention times which qualitatively confirmed their presence.

Cell culture

Human lung adenocarcinoma (A549) cell lines and Kaighn's Modification of Ham's F-12 (F-12K) medium were obtained from American Type Culture Collection (ATCC). A549 NSCLC cells were cultured in F-12K medium, which was supplemented with 10% fetal bovine serum (PAA, Austria) and 1% of 100 µg mL⁻¹ penicillin and streptomycin (Biowest, USA). Cells were grown in a humidified incubator at 37 °C under 5% CO₂.

Animals

Male BALB/C mice (6 weeks old, weighing 19–20 g) were purchased from Faculty of Veterinary Medicine, University Putra Malaysia. Mice were given standard chow and water and kept

in a 12 h light/12 h dark cycle. The animal studies were performed in strict accordance with the Guidelines of the Institutional Animal Care and Use Committee (IACUC) of University Putra Malaysia (protocol approval number: UPM/IACUC/AUP-R016/2013).

In vivo tumour xenograft model

Ten mice were selected randomly and assigned as the healthy control group (I). A549 NSCLC cells (2 × 10⁷) resuspended in 100 µL PBS were injected subcutaneously into the backs of forty mice.¹⁰ When the tumour sizes reached approximately 100 mm³, after 14 days of implantation, the mice were randomly assigned to the following experimental groups and had administered daily by oral gavage for 21 days: (II) saline; (III) erlotinib (50 mg kg⁻¹);¹¹ (IV) 150 mg kg⁻¹ of *M. citrifolia* leaves and (V) 300 mg kg⁻¹ of *M. citrifolia* leaves. The tumour volumes were measured every 3 days using the following formula:

$$\text{Tumour volume (mm}^3\text{)} = a(b^2)/2,$$

where *a* = largest diameter and *b* = smallest diameter.

Mice were sacrificed *via* intraperitoneal injection of ketamine HCl (100 mg kg⁻¹) and xylazine (10 mg kg⁻¹). The tumours were excised and some were snap frozen in liquid nitrogen for gene expression, while others were fixed in 10% formalin and embedded in paraffin for hematoxylin and eosin (H&E) and immunohistochemical (IHC) examination. Blood samples were collected in EDTA coated collection tubes for differential counts. Blood cells were stained using ABBOT reagent and analyzed in an ABBOT Celldyn 3700 (Geliga-SistemSdnBhd, Petaling Jaya, Malaysia).

Immunohistochemistry staining

Immunohistochemistry (IHC) staining was used to evaluate the EGFR expression in the tumour foci of the A549-induced tumours using a light microscope. IHC kits (ChemMate™ DAKO EnVision™ Detection Kit, Peroxidase/DAB, Rabbit/Mouse) were purchased from Dako, Denmark. The primary antibody was the anti-EGFR antibody ab15669 (Abcam; Cambridge, United Kingdom). The tumour tissues were embedded in paraffin blocks which were cut using a microtome into 4 µm sections, deparaffinized and consequently incubated in xylene, absolute ethanol, and 90%, 70% and 50% ethanol for 3 minutes each. They were then treated with sodium citrate (pH 6) and boiled for 10 minutes for de-masking. The slides were rinsed with washing buffer (5 dissolved PBS tablets in 1 L of distilled water with 1 ml of Tween-20 added), followed by blocking with 300 µL of H₂O₂ for 5 minutes. After washing, the processed tissue sections were incubated with primary antibodies (EGFR) overnight at 4 °C. Subsequently, the slides were treated for 1 h with secondary, goat anti-mouse anti-rabbit antibodies conjugated with horseradish peroxidase, and developed with 3,3'-diaminobenzidine. Finally, the tissue sections were rinsed in distilled water, counterstained with Mayrri's hematoxylin and mounted with DPX mounting medium for

microscopic examination. Immunohistograms were taken with a phase contrast microscope (Leica, Wetzlar, Germany). Immunohistochemical staining of the tissue sections was performed in triplicate.

Immunophenotyping analysis of inflammatory cytokines

The isolated lymphocytes from the spleens (the primary site for platelet-reactive T and B cell activation)¹² of the A549-bearing mice after 21 days of treatment were analyzed using flow cytometry. Immunophenotyping was performed to assess the lymphocyte population using a Becton Dickinson (BD) FACS Calibur (BD, Franklin Lakes, New Jersey) using fluorochrome conjugated monoclonal antibodies (Serotec) directed against receptors to CD4+ (PerCP-Cy), CD8+ (APC), CD19+ (PE) and CD335+ (PerCP-Cy) antigens, following the manufacturer's protocol (BD Bioscience). The collected spleen tissues were meshed through a 70 μ m cell strainer with 5 ml of PBS–EDTA–BSA (phosphate buffered saline–ethylenediaminetetraacetic acid–bovine serum albumin). After spin down, the pellets were washed with 3 ml of PBS twice, followed by incubation with 2 ml of lysis buffer (NH_4Cl) at 4 °C for 10 minutes. After washing, the number of cells should not have been more than 2×10^6 cells. The cells were incubated with 5 μ l of dye in ice for 90 minutes, then washed with PBS, and added to 600 μ l of 1% paraformaldehyde. The cells were incubated at 4 °C for 7 days. Cell pellets were suspended in PBS and analyzed by FACS using CellQuest analysis software (BD FACS Canto II, USA).

Gene expression

Tumour RNA was isolated using Trizol (Invitrogen, Carlsbad, CA). A Custom RT² Profiler PCR Array (CAPM11988), RT² SYBR Green qPCR Mastermix, RT² First Strand Kit and RNase-Free DNase Set were purchased from SuperArray Bioscience Corporation (Frederick, MD). A quantitative RT-PCR array for differentially expressed genes was performed utilizing RT² Profiler PCR Array Data Analysis version 3.5 (SABiosciences; Frederick, MD, USA), which normalized to HSP90AB1 (NM_008302) and GAPDH (NM_008084). RT-PCR data is represented as the average relative mRNA gene expression of each experimental group ($n = 3$). Fold change ($2^{(-\Delta\Delta\text{Ct})}$) is defined as the normalized gene expression ($2^{(-\Delta\text{Ct})}$) in the test sample, divided by the normalized gene expression ($2^{(-\Delta\text{Ct})}$) in the control sample. Fold regulation represents fold-changes as biologically meaningful results. Fold change values greater than one indicate a positive- or up-regulation, and the fold-regulation is equal to the fold-change. Fold change values less than one indicate a negative- or down-regulation, and the fold-regulation is the negative inverse of the fold-change. The p values are calculated based on a t -test of the replicate $2^{(-\Delta\text{Ct})}$ values for each gene in the control group and the treatment groups.

Statistical analysis

Data was expressed as the mean \pm the standard deviation (mean \pm SD) of at least three independent experiments; significant differences ($p < 0.05$) were calculated using one-way analysis of variance (ANOVA) and the Duncan test using statistical

analysis IBM SPSS Statistics 21 software. The Student's t -test was used where values of $p < 0.05$ were considered significant.

Results

Fig. 1A shows the tumour volumes that were measured every 3 days, which were most highly suppressed in the animals receiving 300 mg kg^{-1} of the extract ($14.81 \pm 19.06 \text{ mm}^3$), followed by 50 mg kg^{-1} of erlotinib ($36.26 \pm 37.00 \text{ mm}^3$), and 150 mg kg^{-1} of extract ($138.28 \pm 93.91 \text{ mm}^3$) which were significantly smaller compared with the control tumour-induced untreated animals ($288.21 \pm 41.53 \text{ mm}^3$). The 300 mg extract per kg group showed body weight increases that were insignificantly different to the healthy control mice by the 21st day (Fig. 1B).

Fig. 2 shows a good correlation between the tumour EGFR expressed by the A549 NSCLC and their IHC EGFR status, which is in line with reports by other researchers.¹³ Fig. 2A demonstrates the different orientation directions (visible as small aggregated clusters or cord like growth) and forms (variably sized and shaped hyperchromatic nuclei) of the cancer cells, and some unknown cells. The cancer cells secreted copious extracellular matrix to expedite their growth, which appeared as unstructured pinkish proteinacious constituents. The proliferated fibroblast-like tumour cells are disseminated in a twisted whirlpool-like pattern. Fig. 2B displays the EGFR immunohistochemistry stain of the mass extracellular matrix of a fibrosarcoma growth to the antibody, and their dispersed orange-chocolate coloured affirmative responses.

Fig. 3 shows that the untreated tumour induced mice had significantly lower lymphocyte ($3.14 \pm 0.14 \times 10^9 \text{ L}^{-1}$) counts than the healthy mice ($6.08 \pm 0.10 \times 10^9 \text{ L}^{-1}$). Treatment with 300 mg kg^{-1} of the extract significantly increased the total white blood cell (WBC, $9.93 \pm 0.42 \times 10^9 \text{ L}^{-1}$) levels and lymphocyte ($7.98 \pm 0.43 \times 10^9 \text{ L}^{-1}$) counts in the tumour-induced mice. The 50 mg kg^{-1} erlotinib and 150 mg kg^{-1} extract treatments produced significantly lower effects than the 300 mg kg^{-1} extract. Similarly, Fig. 4 shows a highly significant increase in the immune cells (T helper cells, monocytes, macrophages, and dendritic cells), and CD4 markers of $42.45 \pm 0.15\%$; co-receptors for the T cell receptor CD8 biomarker of $27.13 \pm 0.39\%$; B cells (CD19 biomarker) of $26.89 \pm 0.49\%$ and natural killer cell (CD335 biomarker) levels of $2.34 \pm 0.14\%$ from the 300 mg kg^{-1} extract treatment compared with the untreated tumour-induced mice.

Mouse RT-PCR arrays were performed for the tumour tissues. Quantitative RT-PCR analyses were performed using the comparative threshold cycle method to calculate fold change in the gene expression normalized to Gapdh and Hsp90ab1 as the reference housekeeping genes. Table 1 shows that the extract significantly ($p < 0.05$) up-regulated the tumour suppressor gene (phosphatase and tensin homolog, PTEN) and down-regulated the tumour cell proliferation genes such as (i) epidermal growth factor receptor (EGFR), (ii) MDM2 (transformed mouse 3T3 cell double minute 2), (iii) RAF1 (V-raf-leukemia viral oncogene 1), and (iv) MTOR (mechanistic

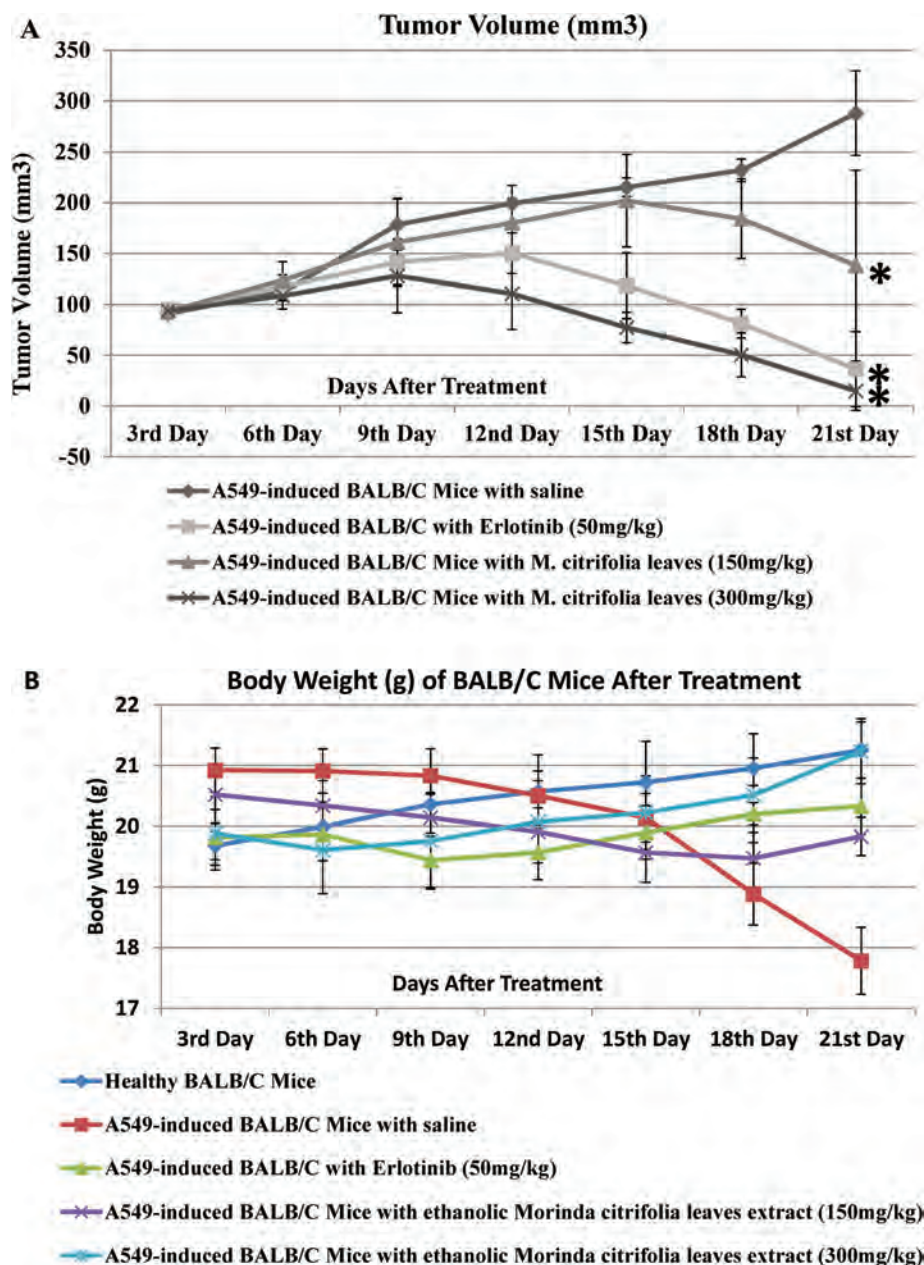


Fig. 1 Effect of *M. citrifolia* leaf extract on the tumour volumes (tumourigenicity) and body weights of the NSCLC-induced mice by comparing untreated and extract-treated or erlotinib-treated mice (mean \pm SD).

target of rapamycin) mRNA expression in the tumour-induced mice. Table 1 also shows that the extract strongly and dose-dependently suppressed the pro-inflammatory COX2 (cyclooxygenase 2) expression (150 mg kg^{-1} : -1.72 -fold, $p = 0.17$; 300 mg kg^{-1} : -4.09 -fold, $p = 0.05$), while 50 mg kg^{-1} of erlotinib did not.

Fig. 5 shows the HPLC profile and analysis of the *Morinda* leaf extract together with the epicatechin and scopoletin standards, run under similar conditions. The profile shows that the epicatechin (3.4%) and scopoletin (2.2%) may be the major bioactive compounds that may have contributed to the effects.

Discussion

NSCLC has distinct morphological and molecular subtypes, usually with EGFR activation and the stimulation of (i) the rat sarcoma (RAS)-mitogen-activated protein kinase 1 (ERK), which controls gene transcription and cell proliferation, and (ii) the phosphoinositide-3-kinase (PI3K)-v-akt murine thymoma viral oncogene homolog 1 (AKT) axes, which induces pro-survival signals.¹⁴ These signalling biomarkers are anticancer targets to induce apoptosis and/or inhibit tumour angiogenesis. However, lung cancer cells always

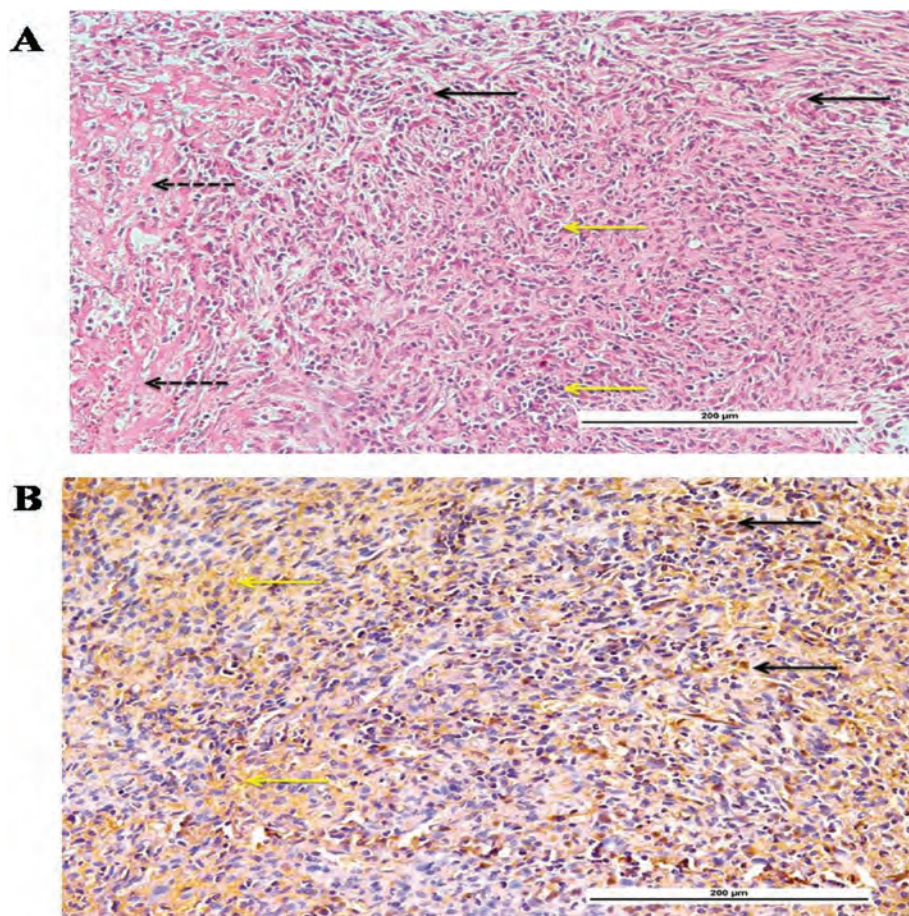


Fig. 2 Photomicrographs of tumours from the mice at the end of the treatment, representative of three different experiments ((A) H&E and (B) IHC, X200). (A) shows the tumour cells oriented in different directions and forms, like small aggregated clusters or cord like growths (yellow arrow) with variably sized and shaped hyperchromatic nuclei and unidentified cells. The abundant extracellular matrix secreted by the tumour cells to facilitate their spread, appeared as an amorphous pinkish pool of proteinacious materials (dashed black arrow). The multiplied fibroblast-like cancer cells are distributed in a warped whirlpool-like shape (black arrow). (B) shows the immunohistochemistry staining of the extracellular matrix ground substance of a fibrosarcoma like tumour mass to an EGFR antibody, and the disseminated golden-brown positive reaction to the antibody in the tissue section background (yellow arrow). Some of the tumour mass cells showed positive reactions to the EGFR as indicated by their deep brown color (black arrow).

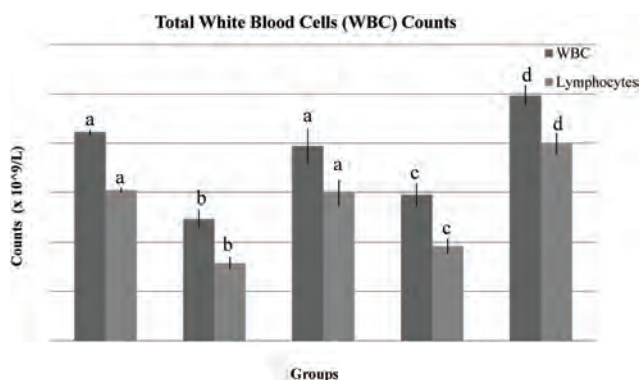


Fig. 3 The white blood cell counts of the different treatment groups. The values are expressed as the mean \pm standard deviation ($n = 3$). Means with different superscript letters within the same graph are significantly different ($p < 0.05$).

stimulate multiple signalling pathways to trigger proliferation and growth.

Scopoletin has been demonstrated to possess weak cytotoxic activities towards various cancer cell lines, including A549 lung cancer, with an IC_{50} higher than $100 \mu M$.¹⁵ Epicatechin is also not known to be an anti-cancer agent. However, epicatechin may enhance the cytotoxic properties of scopoletin, similar to reports that showed (–)-epicatechin enhanced curcumin apoptosis and growth suppression effects in Human Lung Cancer Cells.¹⁶ The presence of epicatechin together with scopoletin in the edible leaf extract may synergistically boost the anti-lung cancer effects of the *M. citrifolia* leaf extract in this situation. Scopoletin was identified as one of the compounds that may be partly responsible for the *Morinda* leaf's anti-angiogenic activity¹⁷ in suppressing tumour growth.

The leaves also reportedly contained Δ^5 sterol β -sitosterol, $\Delta^{5,7}$ sterol campesta-5,7,22-trien-3 β -ol, (+)-catechin, α -ionone,

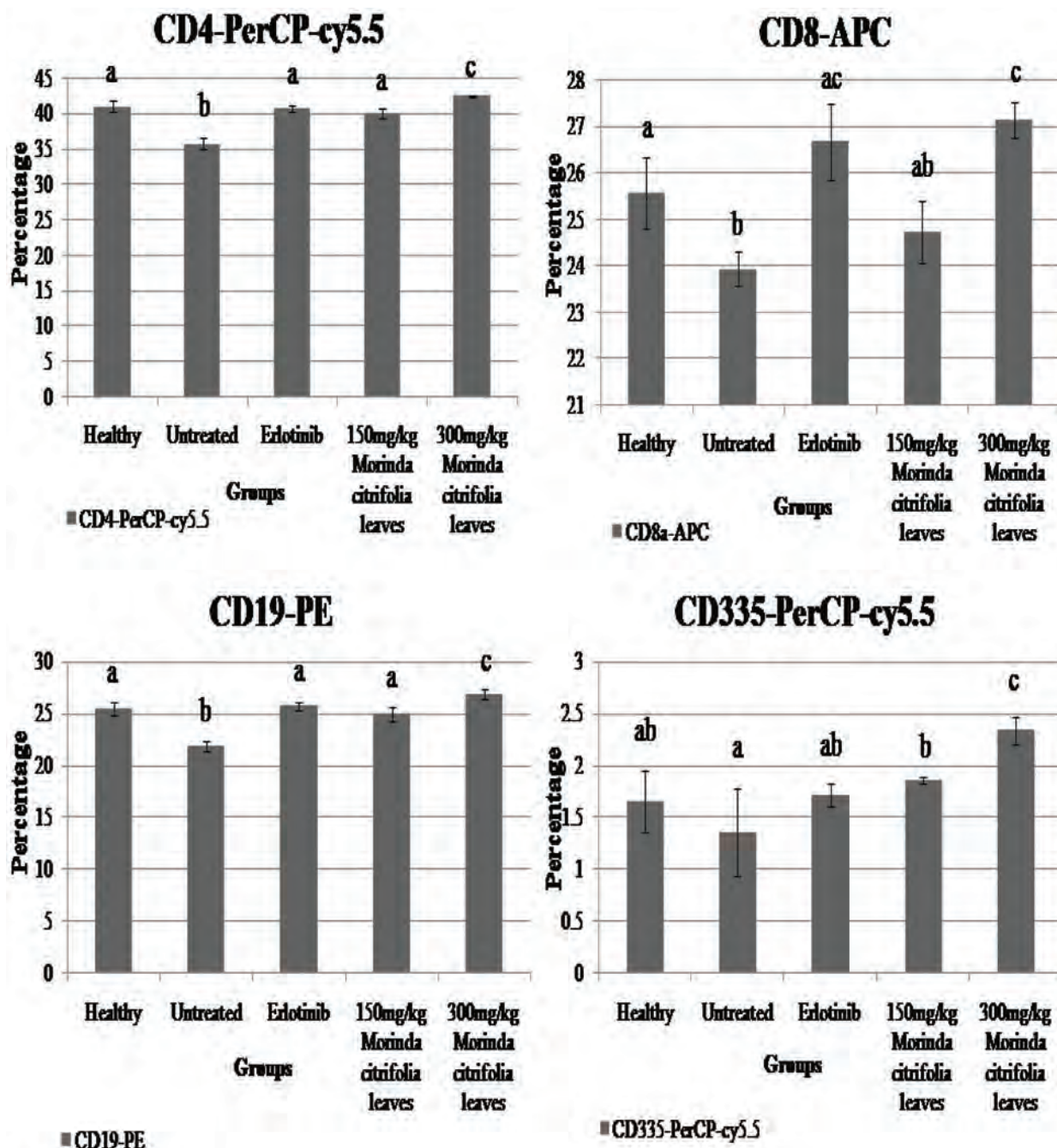


Fig. 4 Immunophenotype analyses of B cells, T cells and natural killer markers in spleen tissue. The values are expressed as mean \pm standard deviation ($n = 3$). Means with different superscript letters within the graph are significantly different ($p < 0.05$).

β -carotene, β -ionone, β -sitosterol, 1,2-dihydro-1,1,6-trimethylnaphthalene, 1,5,15-trimethylmorindol, 2,6,10,14,18,22-tetracosahexaene, 2-methyl-3,5,6-trihydroxyanthraquinone, 2-methyl-3,5,6-trihydroxyanthraquinone-6- O - β -D-xylopyranosyl-(1-6)- β -D-glucopyranoside, 3-hydroxymorindone, 3-hydroxymorindone 6- O - β -D-xylopyranosyl-(1-6)- β -D-glucopyranoside, 3- O -acetylpomolic acid, 4-(3'(R)-hydroxybutyl)-3,5,5-trimethyl-cyclohex-2-en-1-one, 5,6-dihydroxylucidin, 5,6-dihydroxylucidin 3- O - β -D-xylopyranosyl-(1-6)- β -D-glucopyranoside, 5,15-dimethyl-

morindol, 5,15-DMM, 5-methylfurfural, 5-benzofuran carboxylic acid-6-formyl methyl ester, 6,10,14-trimethyl-2-pentadecanone, 13-epi-phaeophorbide a methyl ester, 13-hydroxy-9,11,15-octadecatrienoic acid, 132(R)-hydroxypheophorbide a methyl ester, 13(S)-hydroxypheophorbide a methyl ester, 15¹(R)-hydroxypurpurin-7 lactone dimethyl ester, 15(S)-hydroxypurpurin-7 lactone dimethyl ester, alanine, arginine, aspartic acid, asperuloside, asperulosidic acid, aucubin, barbinervic acid, benzaldehyde, benzeneacetaldehyde, campesta-

Table 1 The mouse RT-PCR array on tumor tissues. Quantitative RT-PCR analysis was performed using the comparative threshold cycle method to calculate fold change in the gene expression normalized to Gapdh and Hsp90ab1 as reference genes

Gene	Accession number	Description	Fold change					
			Erlotinib (50 mg kg ⁻¹)	<i>p</i> value	<i>M. citrifolia</i> leaves extract (150 mg kg ⁻¹)	<i>p</i> value	<i>M. citrifolia</i> leaves extract (300 mg kg ⁻¹)	<i>p</i> value
MDM2	NM_010786	Transformed mouse 3T3 cell double minute 2	−1.25	0.53	−1.16	0.57	−2.96	0.04*
EGFR	NM_007912	Epidermal growth factor receptor	−3.62	0.01*	−1.90	0.09	−2.85	0.03*
RAF1	NM_029780	V-raf-leukemia viral oncogene 1	−2.51	0.00*	−1.50	0.13	−3.41	0.00*
PTEN	NM_008960	Phosphatase and tensin homolog	2.82	0.14	2.42	0.04*	4.23	0.05*
MTOR	NM_020009	Mechanistic target of rapamycin	−2.75	0.03*	−2.22	0.04*	−2.71	0.05*
COX2	NM_011198	Cyclooxygenase-2	−1.38	0.90	−1.72	0.17	−4.09	0.05*

Values represent fold change between the control and treatment groups, and differed significantly at $p < 0.05$, represented by “*”.

5,7,22-trien-3 β -ol, campesterol, citrifolinin A, citrifolinin A-1, citrifolinin Ba, citrifolinin Bb, citrifolinoside A, citrifolinoside B, citrifoside, clethric acid, cycloartenol, cysteine, cystine, deacetyl asperuloside, deacetylasperulosidic acid (DAA), *E*-phytol, epicatechin, geranyl acetone, glutamic acid, glycine, hederagenin, histidine, isoleucine, kaempferol, kaempferol-3-*O*- α -L-rhamnopyranosyl-(1 \rightarrow 6)- β -D-glucopyranoside kaempferol 3-*O*- β -D-glucopyranosyl-(1 \rightarrow 2)- α -L-rhamnopyranosyl-(1 \rightarrow 6)- β -D-galactopyranoside, ketosteroid stigmasta-4-en-3-one, leucine, linoleic acid, lucidin, lucidin 3-*O*- β -D-xylopyranosyl-(1 \rightarrow 6)- β -D-glucopyranoside, methionine, methyl oleate, methyl pheophorbide a, methyl pheophorbide b, methyl plamitate, nicotifloroside, oleanolic acid, oxalic acid, palmitic acid, peucedanocoumarin III, phenylalanine, pheophorbide a, phytic acid, phytol, proline, pteryxin, quercetin, quercetin-3-*O*- α -L-rhamnopyranosyl-(1 \rightarrow 6)- β -D-glucopyranoside, quercetin 3-*O*- β -D-glucopyranoside, quercetin 3-*O*- β -D-glucopyranosyl-(1 \rightarrow 2)- α -L-rhamnopyranosyl-(1 \rightarrow 6)- β -D-galactopyranoside, roseoside II, rotungenic acid, rutin, scopoletin, serine, stigmasta-4-22-dien-3-one, stigmasta-4-en-3-one, stigmasterol, tannic acid, threonine, triterpene cycloartenol, tryptophan, tyrosine, ursolic acid, and valine.^{18,19} Flavonoids such as kaempferols are also reportedly cancer inhibitory.

There are many *in vitro* and *in vivo* reports on the anti-cancer properties of *M. citrifolia* fruit extract²⁰ but very few on the leaf extract and none (to our knowledge) towards lung cancer. There was an *in vivo* study report of the juice extract against S180 tumor cells or Lewis lung carcinoma (LL/2) cells but none were found on NSCLC. The epicatechin and scopoletin rich *M. citrifolia* leaf extract (Fig. 5) demonstrated immunostimulatory effects evidenced by the enhanced total WBC, immune cell CD4, T cell CD8, B cell CD19 and natural killer cell CD335 levels in the blood and spleen. Targeting a single cellular or physiological event alone is usually insufficient to control cancer growth. Additionally, the *M. citrifolia* leaves markedly inhibited cancer cell proliferation, inflammation and angiogenesis *via* mRNA signalling pathways through MDM2/p53, RAF/MEK/ERK, PI3 K/AKT/MTOR, PTEN-dependent and COX2 gene expression. Usually no single component is fully responsible for the activity of a crude leaf extract. Scopoletin

may produce anti-angiogenic effects *via* down-regulating ERK1/2 to inhibit endothelial cell migration and tube formation.²¹ Scopoletin may also induced cell proliferation on normal T lymphocytes without mitogen stimuli *via* protein kinase C (PKC) activation.²²

M. citrifolia leaf extract dose-dependently increased the total WBC, lymphocyte and T cell CD8 and CD4 levels in the tumour-induced mice, demonstrating its strong immune-stimulating effects. The CD8 cytotoxic T cells are important for effective immune defence against cancer, and NSCLC patients with high CD8T cell infiltration have a relatively better survival rate.²³ The CD8T cells need an adequate amount of CD4T cells to fully function *in vivo*.²⁴ *M. citrifolia* leaf extract may help to increase the capacity of T cell specific proliferation and anti-tumour cytotoxicity by releasing perforin, granzymes, granulysin, and interferon gamma (IFN γ)²⁵ to strengthen the CD8T cell-mediated tumour elimination immune response.

The antitumour effects of CD4T cells are dependent on cytokine signalling, especially IFN γ and tumour necrosis factor α (TNF α).²⁶ IFN γ can up-regulate major histocompatibility complex (MHC) molecules; consequently, the tumour recognition is enhanced, resulting in greater tumour cell lysis. The FAS ligand interaction of FAS, a TNF family of receptors, on target cells activates caspases that initiate deoxyribonucleic acid (DNA) fragmentation and apoptosis of cancer cells. The CD4T cells could induce tumour dormancy that prevents tumour escape.²⁷ All data implied that the *M. citrifolia* leaf extract positively affected the activated receptors on the T cells, to enhance the T cell-mediated immune responses of the host towards the unwanted tumour cells.

The *M. citrifolia* leaves also enhanced the CD19 and CD335 in the tumour-induced mice. CD19 is a transmembrane protein expressed on B cells and follicular dendritic cells. The CD19 cell surface expression is lower relative to CD20, but it begins earlier and persists longer through B-cell maturation. CD19 has been validated clinically as a B-cell malignancy target, and enhancing the immune effector functions would be expected to improve the therapeutic efficacy.²⁸

The CD335 immunophenotype is characteristic of the natural killer (NK) cells. This natural cytotoxicity receptor

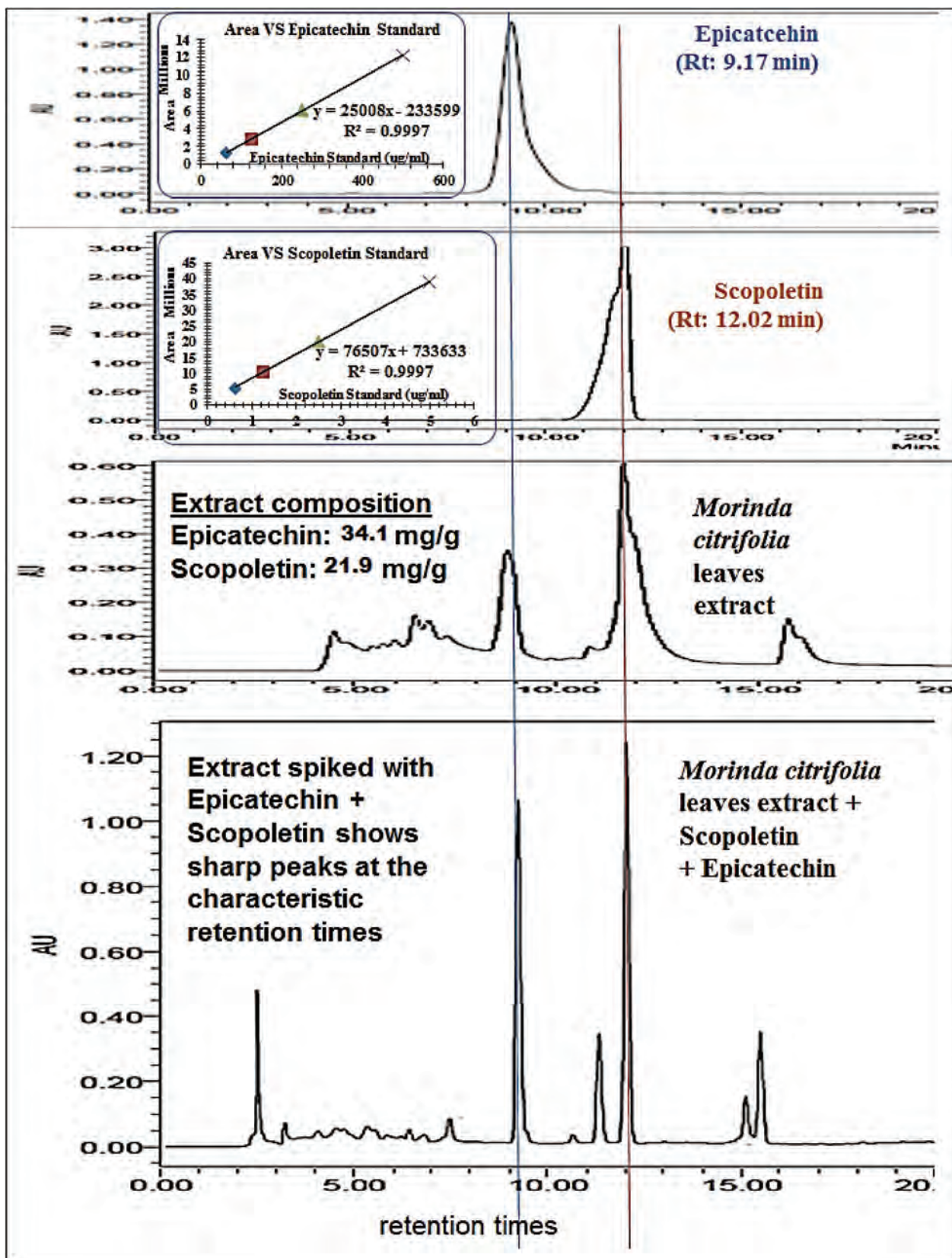


Fig. 5 Qualitative and quantitative HPLC chemical analyses of *M. citrifolia* leaf 50% ethanol extract.

(NCR) family member is present in human and murine NK cell markers for bone marrow, blood and the spleen. A higher CD335 expression correlates with stronger cytotoxicity against tumour cell lines.²⁹ T cells can be selectively induced to express CD335, through a functional PI3 K/AKT signalling on stimulation with γ c cytokines and T cell receptor (TCR) agonists.³⁰ The adaptive immunity is coordinated by the antigen-specific T and B lymphocytes and directly kills the tumour cells *via* the cytotoxic T lymphocytes (CTLs) in combination with the cytokine- and antibody-mediated tumour cell lysis.³¹

This study demonstrates that the epicatechin and scopoletin rich *M. citrifolia* leaves help suppress the epidermal growth factor receptor EGFR, which is critical in tumour proliferation, invasion and metastasis and may be useful as a complementary functional food against cancer. The A549 cells in NSCLC over-express EGFR³² (high brown scale IHC staining and strong positive signal by DAB visualization) and the epicatechin and scopoletin rich extract dose-dependently suppressed this in this mammalian model.

EGFR and COX2 have related signalling pathways that can interact to affect cellular proliferation, migration and invasion.³³ *M. citrifolia* leaf extract significantly decreased the tumour tissue COX2 levels *in vivo*, as has been similarly reported for green tea extract *in vitro*.³⁴ In cancer, COX2 overexpression is possibly due to several mechanisms,³⁵ such as, (i)

intrinsic peroxidase activity due to increased mutagen production; (ii) enhanced prostaglandin production stimulated by epithelial cell proliferation; (iii) increased anti-apoptotic protein (B-cell lymphoma 2, BCL2) levels; (iv) pro-angiogenic factor production; (v) enhanced invasiveness by matrix metalloproteinases and urokinase plasminogen activation; and (vi) immune suppression.

The epicatechin and scopoletin rich *M. citrifolia* leaf extract dose-dependently increased the tumour suppressor PTEN levels in the mice's lung tumours, comparable to green tea extract in lung cancer cells.³⁶ PTEN regulates cell survival, proliferation, invasion and angiogenesis by acting as a lipid phosphatase that antagonizes PI3K signalling *via* dephosphorylating phosphatidylinositol (3,4,5)-trisphosphate (PIP3) back to phosphatidylinositol (4,5)-bisphosphate (PIP2). Reduced PTEN expression was associated with a poor clinical outcome in NSCLC.³⁷ Loss of PTEN permits activated AKT to phosphorylate the intracellular protein BAD (Bcl-2-associated death promoter), resulting in the release of the anti-apoptotic protein BCL2, which then leads to cancer cell survival.³⁸ The epicatechin and scopoletin rich leaf extract may possibly be used alone or together with other chemotherapeutic agents for PTEN mutant cancer therapy.

The epicatechin and scopoletin rich *M. citrifolia* leaf extract dose-dependently suppressed MTOR, which is an attractive cancer therapy target because its inhibition could reduce poss-

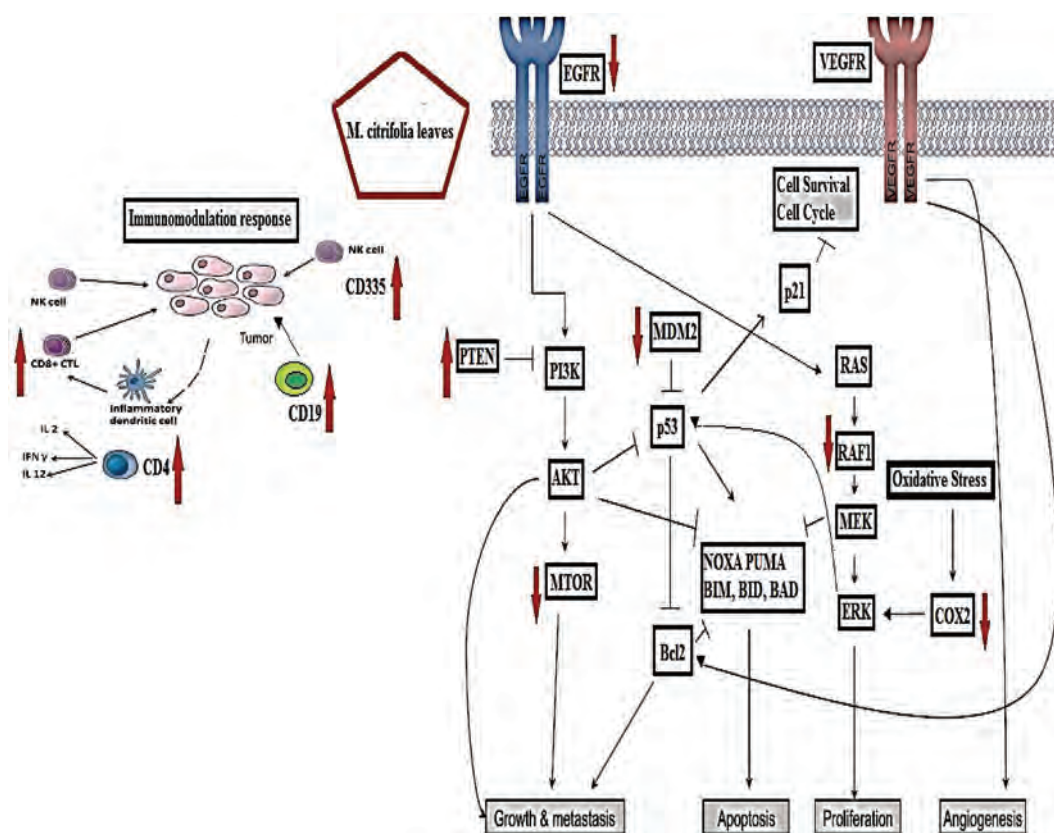


Fig. 6 Proposed model of *M. citrifolia* leaf extract mechanism of action for anti-proliferative and immunomodulation effects against lung adenocarcinoma *in vivo*.

ible side effects associated with the inhibition of upstream PI3 K/AKT signalling molecules. The PI3 K/AKT pathway is involved in broader biological functions including glucose signalling.³⁹

The epicatechin and scopoletin rich *M. citrifolia* leaf extract also dose-dependently inhibited cancer cell proliferation by suppressing MDM2 gene expression. MDM2 negatively controls pro-apoptosis p53 stability, function and concentration by (i) preventing p53 transcription through binding *via* protein-protein interactions to the p53 N-terminal transcription activation domain, (ii) promoting p53 degradation by ubiquitin dependent proteasomal degradation and acting as an E3 ubiquitin ligase, and (iii) causing nuclear export of p53 into the cell cytoplasm, away from its action site.⁴⁰ The p53-dependent apoptosis is induced by the caspase proteases and death receptors and occurs through pro-apoptotic proteins including BAX (BCL2-associated X protein), NOXA (phorbol-12-myristate-13-acetate-induced protein 1), and PUMA (p53 upregulated modulator of apoptosis).⁴¹ The epicatechin and scopoletin rich *M. citrifolia* leaf extract further dose-dependently inhibits the MAPK pathway through the suppression of the RAF1 marker to produce anti-proliferative effects, and the suppression of their downstream targets: MEK and ERK. Human small cell lung cancer (SCLC) growth is partially dependent on signalling by RAF1.⁴² The disruption of RAF1 expression by the extract could help inhibit angiogenesis and the pro-survival of the endothelial cells because the PKC/RAF/MEK/ERK signalling pathway is involved in the vascular endothelial growth factor/vascular endothelial growth factor receptor (VEGF/VEGFR) dimerization and activation.^{40,43} The proposed model for the epicatechin and scopoletin rich *M. citrifolia* leaf extract mechanism of action for anti-proliferative and immune-stimulating effects against lung adenocarcinoma *in vivo* is summarised in Fig. 6.

Conclusion

The evidence demonstrated that the epicatechin and scopoletin rich *M. citrifolia* leaf extract may be used as a functional food and complementary therapy to suppress lung cancer by stimulating the immune responses and modulating multiple cancer cell gene signalling pathways against cancer cell proliferation and towards apoptosis, without producing detectable undesirable effects. The extract suppressed key inflammatory markers and inhibited various molecular and cellular markers involved in proliferation and angiogenesis, suggesting a mode of action targeting, as proposed in Fig. 6. The epicatechin and scopoletin rich *M. citrifolia* leaves may be used as a complementary/adjunct therapy or functional food to help fight lung cancer or adenocarcinoma.

Conflict of interest

The authors declare that they currently have no conflict of interest in the research.

Acknowledgements

This study is supported by the Herbal Development Office, Ministry of Agriculture (Grant No. NH05135009).

References

- 1 A. Jemal, F. Bray and M. Center, *CA-Cancer J. Clin.*, 2011, **61**, 69–90.
- 2 S. Spiro, N. Tanner, G. Silvestri, S. Janes, E. Lim, J. Vansteenkistes and R. Pirker, *Respirology*, 2010, **15**, 44–50.
- 3 K. Politi, P. Fan, R. Shen, M. Zakowski and H. Varmus, *Dis. Models Mech.*, 2010, **3**, 111–119.
- 4 M. Edelman, L. Hodgson and X. Wang, *J. Clin. Oncol.*, 2012, **30**, 2019–2020.
- 5 K. Chen, M. Weng and J. Lin, *Biochem. Pharmacol.*, 2007, **73**, 215–227.
- 6 B. Nayak, S. Sandiford and A. Maxwell, *Evidence-Based Complementary Altern. Med.*, 2009, **6**, 351–356.
- 7 B. West, H. Tani, A. Palu, C. Tolson and C. Jensen, *J. Sci. Food Agric.*, 2007, **87**, 2583–2588.
- 8 A. Lagarto, V. Bueno and N. Merino, *J. Interact. Ethnopharmacol.*, 2013, **2**, 15–22.
- 9 S. Deng, B. West and C. Jensen, *Food Chem.*, 2010, **122**, 267–270.
- 10 X. Xu and G. D. Prestwich, *Cancer*, 2010, **116**, 1739–1750.
- 11 J. Clark, M. Provenzano, H. Diggelmann, N. Xu, S. Hansen and M. Hansen, *Otol. Neurotol.*, 2008, **29**, 846–853.
- 12 M. Kuwana, Y. Okazaki, J. Kaburaki, Y. Kawakami and Y. Ikeda, *J. Immunol.*, 2002, **168**, 3675–3682.
- 13 J. Kurai, H. Chikumi, K. Hashimoto, K. Yamaguchi, A. Yamasaki, T. Sako, H. Touge and H. Makino, *Clin. Cancer Res.*, 2007, **13**, 1552–1561.
- 14 T. Mitsudomi and Y. Yatabe, *FEBS J.*, 2010, **277**, 301–308.
- 15 X. Cai, J. Yang, J. Zhou, W. Lu, C. Hu, Z. Gu, J. Huo, X. Wang and P. Cao, *Bioorg. Med. Chem.*, 2013, **21**, 84–92.
- 16 A. Saha, T. Kuzuhara, N. Echigo, M. Suganuma and H. Fujiki, *Cancer Prev. Res.*, 2010, **3**, 953–962.
- 17 H. Beh, L. Seow, M. Asmawi, A. Abdul Majid, V. Murugaiyah, N. Ismail and Z. Ismail, *Nat. Prod. Res.*, 2012, **26**, 1492–1497.
- 18 S. Deng, B. West, A. Palu and C. Jensen, *Phytochem. Anal.*, 2011, **22**, 26–30.
- 19 B. West and B. Zhou, *J. Nat. Med.*, 2008, **62**, 485–487.
- 20 M. Wang and C. Su, *Ann. N. Y. Acad. Sci.*, 2001, **952**, 161–168.
- 21 R. Pan, Y. Dai, J. Yang, Y. Li, X. Yap and X. Xia, *Drug Dev. Res.*, 2009, **70**, 214–219.
- 22 M. Manuele, G. Ferraro, M. Arcos, P. López, G. Cremaschi and C. Anesini, *Life Sci.*, 2006, **79**, 2043–2048.
- 23 E. Verdegaa, C. Hoogstraten, M. Sandel, P. Kuppen, A. Brink, F. Claas, M. Gorsira, F. Roggen and S. Roggen, *Cancer Immunol. Immunother.*, 2007, **56**, 587–600.
- 24 R. Bos and L. Sherman, *Cancer Res.*, 2010, **70**, 8368–8377.

- 25 K. Murphy, *Janeway's immunobiology*, Garland Science, 8th edn, 2011.
- 26 A. Smith and S. Andreansky, *Med. Sci.*, 2013, **2**, 1–22.
- 27 N. Müller-Hermelink, H. Braumüller, B. Pichler, T. Wieder, R. Mailhammer, K. Schaak and K. Ghoreschi, *Cancer Cell*, 2008, **13**, 507–518.
- 28 R. Bargou, E. Leo, G. Zugmaier, M. Klinger, M. Goebeler, S. Knop, R. Noppeney and A. Viardot, *Science*, 2008, **321**, 974–977.
- 29 A. G. Freud, S. Zhao, S. Wei, G. M. Gitana, H. F. Molina-Kirsch, S. K. Atwater and Y. Natkunam, *Am. J. Clin. Pathol.*, 2013, **140**, 853–866.
- 30 D. Correia, M. Fogli, K. Hudspeth, M. da Silva, D. Mavilio and B. Silva-Santos, *Blood*, 2011, **118**, 992–1001.
- 31 K. Visser, A. Eichten and L. Coussens, *Nat. Rev. Cancer*, 2006, **6**, 24–37.
- 32 A. Yasmeen, T. Bismar and A. Moustafa, *Future Oncol.*, 2006, **2**, 765–781.
- 33 K. Krysan, K. Riedl, S. Sharma, M. Dohadwala and S. Dubinett, *Cancer Res.*, 2004, **65**, 6275–6281.
- 34 Q. Lu, Y. Jin, J. Mao, Z. Zhang, D. Heber, S. Dubinett and J. Rao, *Biochem. Biophys. Res. Commun.*, 2012, **427**, 725–730.
- 35 V. Neergheen, T. Bahorun, E. Taylor, L. Jen and O. Aruoma, *Toxicology*, 2010, **278**, 229–241.
- 36 X. Liu, D. Zhang, W. Zhang, X. Zhao, C. Yuan and F. Ye, *Nutr. Cancer*, 2011, **63**, 466–475.
- 37 G. Bepler, S. Sharma, A. Cantor, A. Gautam, E. Haura and G. Simon, *J. Clin. Oncol.*, 2004, **22**, 1878–1885.
- 38 Q. Li, G. Wang, F. Huang, M. Banda and E. Reed, *J. Pharm. Pharmacol.*, 2010, **62**, 1018–1027.
- 39 J. Crowell, V. Steele and J. Fay, *Mol. Cancer Ther.*, 2007, **6**, 2139–2148.
- 40 J. Javid, A. Mir, I. Ahamad, S. Farooq, P. Yadav, M. Zuberi, M. Masroor and P. Ray, *J. Cancer Sci. Ther.*, 2012, **04**, 341–346.
- 41 J. Ju, M. Jeon, W. Yang, K. Lee, H. Seo and I. Shin, *J. Ethnopharmacol.*, 2011, **133**, 126–131.
- 42 S. Takeuchi, K. Fukuda, S. Arai, S. Nanjo, K. Kita, T. Yamada, E. Hara, H. Nishihara, H. Uehara and S. Yano, *Int. J. Cancer*, 2016, **138**, 1281–1289.
- 43 T. Bhat and R. Singh, *Food Chem. Toxicol.*, 2008, **46**, 1334–1345.